JOURNAL OF GUIDANCE, CONTROL, AND DYNAMICS
Vol. 37, No. 6, November–December 2014

Engineering Notes

Safety Margins for Flight Through Stochastic Gusts

Johnhenri R. Richardson,* Pierre T. Kabamba,† Ella M. Atkins,‡ and Anouck R. Girard§
University of Michigan, Ann Arbor, Michigan 48109

DOI: 10.2514/1.G000299

I. Introduction

WIND disturbances are a common factor in aviation accidents. Among 126 airplane accidents that occurred between 1979 and 2009 involving loss of control in flight, 14% listed windshear, turbulence, or thunderstorms as a cause or contributing factor. Moreover, 86% of the accidents initiated by atmospheric disturbances led to an upset flight condition, which usually entails an excursion of the aircraft state outside of the flight envelope. Sixty-four percent of these accidents also involved inappropriate crew response [1].

The flight envelope, the set of airspeeds, altitudes, flight-path angles, and bank angles at which an airplane can maintain steady flight, is useful for identifying when an airplane is prone to loss of control. Airplanes are at a higher risk of loss of control when flying in unstable flight states. Most airplanes are designed to fly stably or stabilizably when flying steadily; therefore, flight states in the steady flight envelope are generally not conducive to loss of control. In prior work, the authors presented safety margins and adjusted flight envelopes called stationary flight envelopes for airplane flight through stochastic gusts [2]. Those margins and envelopes were primarily based on the instantaneous probability of exceeding the steady flight envelope, which also corresponds to the fraction of time spent outside the steady flight envelope.

This Note connects several probabilistic safety margins for airplane flight in turbulence, including the instantaneous probability used in the authors' prior work [2]. The safety margins, which are various measures related to the probability of a stochastic process deviating far from its mean value, include 1) the frequency of exceedance, which is the rate at which a stochastic process exceeds a given threshold; 2) the residence time, which is the average time at which a stochastic process exceeds a given threshold for the first time; 3) the logarithmic residence time, which is a dimensionless version of the residence time defined for thresholds far from the mean; 4) the instantaneous probability of exceedance, which is the probability that a stochastic process exceeds a given threshold at time t that, for an ergodic process, is also the fraction of time spent beyond the threshold; 5) the probability of exceedance at time t, which is the probability that a stochastic process has exceeded a given threshold at or before time t; and 6) the probability of exceedance per unit time, which is the probability of exceedance at time t divided by t. These safety margins are applied to the problem of airplane flight through stochastic wind gusts, where the exceedance thresholds are chosen to be the constraints that define the steady flight envelope.

This Note expands upon work by Hoblit on frequency of exceedance [3] to show how to compute the probability per unit time of exceeding the flight envelope, the residence time within the flight envelope, and the logarithmic residence time within the flight envelope. This Note also shows that the logarithmic residence time derived from the frequency of exceedance equals the logarithmic residence time derived by Meerkov and Runolfsson [4] for linear time-invariant systems driven by white noise. The Note concludes that the dimensional and dimensionless measures of safety complement one another to understand the hazard posed by flight through stochastic gusts.

Section II presents the dynamic model of airplane flight through stochastic gusts. Section III shows how to compute the probability per unit time of exceeding a threshold and the residence time within that threshold. Section IV introduces the logarithmic residence time and shows that two disparate methods to compute it give the same result. Finally, Sec. V presents a numerical example related to exceeding the steady flight envelope in turbulence that is validated in simulation in Sec. VI.

II. Linearized Airplane Dynamics in Stochastic Gusts

The authors' prior work [2] derives linearized airplane flight dynamics driven by stochastic gusts expressed in state space form, both with and without feedback control [5]. The result is a linear time-invariant (LTI) system of differential equations linearized around a reference steady flight state. The system's state variables are the airplane linear and angular velocity perturbations δv_c and $\delta\omega$, as well as the Euler angle perturbations $\delta\epsilon$ [5]. The state variables also include the states ξ_w of a prefilter. This prefilter yields the wind gust linear and angular velocity perturbations.

The system has two inputs. The first input is a white noise disturbance $d(t)$ with covariance matrix D that drives the prefilter. Appropriate choice of the prefilter and white noise input yields wind velocity perturbations for which the power spectral density matches that of the Dryden wind turbulence model [6] or approximates that of the von Kármán wind turbulence model [7], as specified by U.S. Department of Defense standards [8]. The other input is the airplane control surface deflections δc, a vector containing the aileron, elevator, and rudder control inputs δ_a, δ_e, and δ_r, respectively.

The linearized dynamics can be expressed compactly as

$$\dot{x} = Ax + B\delta c + Ed(t) \tag{1}$$

$$x = \begin{pmatrix} \delta v_c \\ \delta\omega \\ \delta\epsilon \\ \xi_w \end{pmatrix}, \qquad \delta c = \begin{pmatrix} \delta_a \\ \delta_e \\ \delta_r \end{pmatrix} \tag{2}$$

where A, B, and E are the state, input, and disturbance matrices, respectively. Assuming that this LTI system is driven by zero-mean Gaussian, ergodic, stationary white noise, the state variables are themselves zero-mean Gaussian, ergodic, and stationary random processes. An output $y = Cx$ can be chosen for the system, where C

Received 27 September 2013; revision received 28 January 2014; accepted for publication 30 January 2014; published online 9 May 2014.

*Ph.D. Candidate, Applied Physics Program, 450 Church Street; jhrr@umich.edu. Student Member AIAA.

†Professor, Department of Aerospace Engineering, 1320 Beal Avenue; kabamba@umich.edu.

‡Associate Professor, Department of Aerospace Engineering, 1320 Beal Avenue; ematkins@umich.edu. Associate Fellow AIAA.

§Associate Professor, Department of Aerospace Engineering, 1320 Beal Avenue; anouck@umich.edu. Member AIAA.

is the output matrix. While this Note considers only single output systems, the results are generalizable. The variance of the output is

$$\sigma_y^2 = C\bar{P}C^T \tag{3}$$

where $\bar{P}$ is the covariance matrix of the state vector and the finite, unique, positive definite solution of the Lyapunov equation

$$A\bar{P} + \bar{P}A^T + EDE^T = 0 \tag{4}$$

If the chosen output is the perturbation of some quantity that is constrained in steady flight, such as the true airspeed, the angle of attack, or the normal load factor, then the dynamics and statistics of the output can characterize flight envelope excursions. In prior work [2], the authors note the relationship between the standard deviation of a Gaussian distribution, the instantaneous probability of exceeding the flight envelope, and the fraction of time spent outside the flight envelope [5]. However, current Federal Aviation Administration guidance on computing failure probabilities relies on the probability per flight hour of encountering a hazard [9]. An additional measure that quantifies whether a hazard will be encountered is the residence time: the expected time until a hazard is first encountered. The remaining sections show how to compute the probability per unit time and the residence time for the airplane flight dynamics problem described in this section.

III. Residence Time and Probability per Unit Time Computation from Frequency of Exceedance

For large deviations of a random process, the probability per unit time of exceeding a threshold is closely related to the probability of exceeding the threshold in a given time interval. Chapter 4 of Hoblit's text describes how to compute these probabilities for perturbed variables in the case of airplane dynamics driven by stationary, Gaussian models of turbulence [3]. His method involves determining the frequency with which a Gaussian random process exceeds some threshold, using that frequency as the rate for a Poisson process that counts the number of threshold crossings of the Gaussian random process, and computing the probability that the first jump of the Poisson process occurs at time t. Similar approaches are used in the environmental sciences to assess the risk posed by intense storms [10] and earthquakes [11]. This section expands upon Hoblit's method by providing details about the Poisson process used to compute the probabilities and by showing how to compute the residence time of the process between two thresholds [3].

Rice [12] shows that, for a zero-mean scalar, Gaussian random process y with variance σ_y^2, power spectral density $\Phi_y(f)$, and some threshold $y_{\max} > 0$, the frequency of exceedence of the threshold is

$$N(y_{\max}) = N_0 e^{-(y_{\max}^2/2\sigma_y^2)} \tag{5}$$

Rice [12] defines the frequency of exceedance as the number of threshold upcrossings per unit time. A threshold upcrossing is an event that occurs when the instantaneous value of the random process changes from being less than the threshold value to being greater than the threshold value. N_0 is the number of upcrossings of zero per unit time and can be computed from the power spectral density of the random process

$$N_0 = \sqrt{\frac{\int_0^\infty f^2 \Phi_y(f)\,\mathrm{d}f}{\int_0^\infty \Phi_y(f)\,\mathrm{d}f}} \tag{6}$$

The integral in the numerator of N_0 is problematic because it does not converge for either the Dryden or von Kármán models of continuous gusts. This makes it difficult or impossible to compute accurate values of N_0 for gust loads, although Hoblit presents standard methods to approximate N_0 for gust loads [3].

Because of the symmetry of the Gaussian distribution, the frequency of crossing $-y_{\min} < 0$ with negative slope is the same after substituting $y_{\min}$ for $y_{\max}$ in Eq. (5). Expressing the threshold in terms of standard deviations, $y_{\max} = k_{\max}\sigma_y$,

$$N(k_{\max}) = N_0 e^{-(k_{\max}^2/2)} \tag{7}$$

According to Hoblit [3], for $k_{\max} > 2$, this frequency of exceedance is a good approximation for the average number of peaks that exceed $y_{\max}$ per unit time on sample paths of y.

Note that, whether counting upcrossings of the threshold or peaks that exceed the threshold, this use of the frequency of exceedance assumes that each exceedance is a single, isolated event. In Sec. VI, the gust response is observed to have high frequency components that, during the infrequent instances when the stochastic process exceeds the threshold, cause the threshold to be crossed several times in rapid succession before the process reverts to the mean.

For many types of stochastic processes, including Gaussian processes, as the threshold whose peaks are being counted grows arbitrarily, the number of peaks that have occurred converges to a Poisson process. The Poisson process interarrival times are exponentially distributed random variables with a rate equal to $N(y_{\max})$ [13]. Assuming the number of peaks grows as a Poisson process, the probability that at time t no peak in excess of the threshold has occurred is $e^{-N(y_{\max})t}$ [14]. Its complement is the probability of exceedance at time t: the probability that at least one peak has exceeded the threshold by time t,

$$p_{\text{ex}}(t) = 1 - e^{-N(y_{\max})t} \tag{8}$$

For small $N(y_{\max})t$, as in the case of large deviations of y from the mean,

$$p_{\text{ex}}(t) \approx N(y_{\max})t \tag{9}$$

and $N(y_{\max})$ is approximately equal to the probability of exceedance per unit time, $p_{\text{ex}}(t)/t$.

Assume that $y(t)$ is a zero-mean stochastic process. Define the first passage time of $y(t)$ from within the thresholds $y_{\max} > 0$ and $-y_{\min} < 0$ as

$$\tau(y_0) = \inf\{t \geq t_0\colon y(t) \in \{-y_{\min}, y_{\max}\} \mid -y_{\min} < y_0 < y_{\max}\} \tag{10}$$

where $y_0 = y(t_0)$, and henceforth t_0 is assumed to be 0. Define this time's mean

$$\bar{\tau}(y_0) = E[\tau(y_0)|y_0] \tag{11}$$

as the residence time. Equivalently, a residence time can be found for $-y_{\min} < y < \infty$ and a separate residence time can be found for $-\infty < y < y_{\max}$. The smaller of the two thresholds, $\min(y_{\min}, y_{\max})$, yields the smaller of the two times, which is the residence time for $-y_{\min} < y < y_{\max}$.

From the preceding discussion, if $y_{\max}$ and $y_{\min}$ are arbitrarily large, then the residence time is also the expected time for the first jump of the Poisson process counting peaks in excess of the smaller threshold. The expected time for the first jump of a Poisson process is the mean of its interarrival times' exponential distribution, which in this case is the inverse of the frequency of exceedance

$$\bar{\tau} = N^{-1}(\min(y_{\min}, y_{\max})) \tag{12}$$

IV. Logarithmic Residence Time

Another measure to quantify when a stochastic process leaves a given set is the logarithmic residence time. This section shows for the first time that two disparate methods of computing the logarithmic residence time give the same result. First, the section reviews definitions and a theorem from work by Meerkov and Runolfsson on aiming control that shows how to compute the logarithmic residence time for LTI systems driven by white noise [4,15]. Their work also derives control laws to control the logarithmic residence time. Second, this section shows that a logarithmic residence time can be formulated from the frequency of exceedance of a stochastic process and that the two logarithmic residence times are the same.

Consider a LTI system modeled in state-space form:

$$\dot{x} = Ax + \varepsilon Ed \tag{13a}$$

$$y = Cx \tag{13b}$$

where $x \in \mathbb{R}^n$; $y \in \mathbb{R}^p$; d is a zero-mean, stationary, Gaussian white noise process with covariance matrix D; ε is a small, positive parameter; and C has rank p. Define a domain $\Psi \subset \mathbb{R}^p$ that contains the origin and has a smooth boundary $\partial\Psi$. Assume that $x_0 = x(0) \in \Omega_0 \triangleq \{x \in \mathbb{R}^n | y = Cx \in \Psi\}$. Denote the output $y(t)$ in Eq. (13) with initial condition x_0 as $y(t, x_0)$. Define the first passage time of the output $y(t, x_0)$ from Ψ as

$$\tau^{\varepsilon}(x_0) = \inf\{t \geq 0\colon\ y(t, x_0) \in \partial\Psi | y(t_0, x_0) \in \Psi\} \tag{14}$$

and call its mean

$$\bar{\tau}^{\varepsilon}(x_0) = E[\tau^{\varepsilon}(x_0)|x_0] \tag{15}$$

the residence time. Large deviations theory offers asymptotic approximations of these times for small ε.

Theorem 1: 1) A is Hurwitz and 2) the pair (A, E) is completely controllable. Then, uniformly for all x_0 belonging to compact subsets of $\Omega = \{x_0 \in \mathbb{R}^n | Ce^{At}x_0 \in \Psi, t \geq 0\}$,

$$\lim_{\varepsilon \to 0} \varepsilon^2 \ln \bar{\tau}^{\varepsilon}(x_0) = \hat{\mu}(\Psi) \tag{16}$$

where

$$\hat{\mu}(\Psi) = \min_{y \in \partial\Psi} \frac{1}{2} y^T P^{-1} y \tag{17}$$

$$P = C\bar{P}C^T \tag{18}$$

and $\bar{P}$ is the positive definite solution of the Lyapunov equation

$$A\bar{P} + \bar{P}A^T + EDE^T = 0 \tag{19}$$

This theorem is proven by Meerkov and Runolfsson [15]. The constant $\hat{\mu}$ is referred to as the logarithmic residence time in Ψ.

Consider the special case where y is scalar. The covariance matrix P simplifies to the variance σ_y^2; the domain Ψ simplifies to the real interval $[-y_{\min}, y_{\max}]$, where $y_{\min}$, $y_{\max} > 0$; the boundary $\partial\Psi$ simplifies to the two real numbers $\{-y_{\min}, y_{\max}\}$; and the logarithmic residence time simplifies to

$$\hat{\mu}(\Psi) = \frac{\min(y_{\min}, y_{\max})^2}{2\sigma_y^2} \tag{20}$$

This special case is analogous to the flight dynamics model described in Sec. II, with the addition of control inputs in the flight dynamics model and the addition of the parameter ε to the present model to quantify the relative magnitude of the disturbance. Meerkov and Runolfsson, in showing how to control the logarithmic residence time, show how to incorporate control inputs into the present model [4,15].

The boundary $\partial\Psi$ can be defined relative to the standard deviation of y: $y_{\min} = k_{\min}\sigma_y$, $y_{\max} = k_{\max}\sigma_y$. Substituting into Eq. (20),

$$\hat{\mu}(\Psi) = \frac{1}{2}\min(k_{\min}, k_{\max})^2 \tag{21}$$

The logarithmic residence time for scalar output is proportional to the square of the number of standard deviations between the mean, which is zero, and the boundary closest to the mean. The authors use the number of standard deviations between the flight state and the steady flight envelope boundary as the primary safety margin in their prior work [2]. Equation (21) shows this safety margin to be equivalent to using the logarithmic residence time.

The residence time can be approximated from the logarithmic residence time as

$$\bar{\tau}^{\varepsilon} \approx c(\varepsilon)e^{\hat{\mu}/\varepsilon^2} \tag{22}$$

Meerkov and Runolfsson specify the normalization that determines the preexponential factor $c(\varepsilon)$ but never compute it, relying on the dimensionless logarithmic residence time for all of their applications [4].

The same logarithmic residence time can be found using the frequency of exceedance method described in Sec. III. Normalizing the residence time in Eq. (12) by N_0 and taking the natural log,

$$\hat{\mu} = \ln\left(\frac{N_0}{N(y_{\max})}\right) = \frac{\min(y_{\min}, y_{\max})^2}{2\sigma_y^2} \tag{23}$$

which is the same logarithmic residence time derived from the dynamic model of Meerkov and Runolfsson [4,15]. The authors speculate that, under appropriate assumptions, the preexponential factors $c(\varepsilon)$ and N_0 are also the same; in that case, the residence times from the two methods are also equal.

V. Numerical Example of a Navion in Turbulence

The authors' prior work included a numerical example of a Navion performing various steady flight maneuvers in turbulence [2]. The previous work computed the variances of the true airspeed and normal load factor for these maneuvers. Additionally, it presented safety margins and stationary flight envelopes based on these variances [2,5]. This section expands upon the steady level longitudinal flight in turbulence example from the authors' previous work [2] to include the logarithmic residence time within the steady flight envelope $\hat{\mu}$, the residence time within the steady flight envelope $\bar{\tau}$, and the probability per unit time of exceeding the steady flight envelope, which equals the frequency of exceedance N.

In the example, a Navion is attempting steady level longitudinal flight in moderate turbulence with a reference true airspeed of 102 ft/s at an altitude of 16,500 ft. This is an unusual state of operation for a Navion, since it is so close to stall at high altitude, but it is in the flight envelope and provides a good illustration. Details on the Navion and turbulence models are available in the prior work [2]. In that example, the variance of the true airspeed perturbations $\sigma_{v_t}^2$, and therefore the true airspeed, is 15 ft^2/s^2.

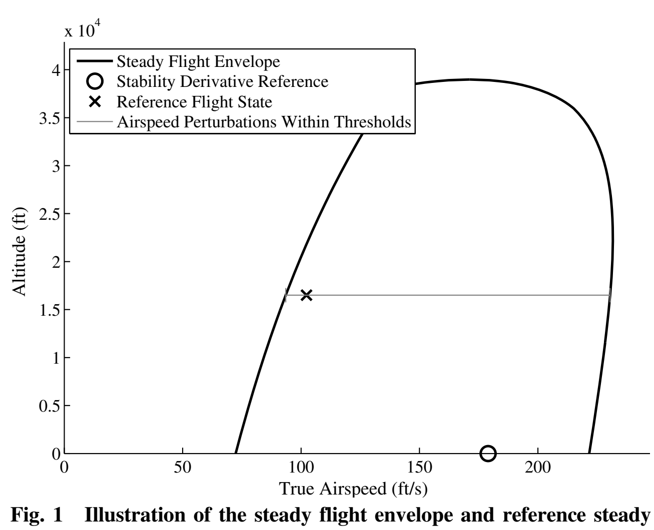

Fig. 1 Illustration of the steady flight envelope and reference steady flight state. Also shown is the reference state for the Navion's stability derivatives.

Table 1 Estimated and simulated values of various airspeed statistics quantifying the probability of a Navion in moderate turbulence exceeding the stall boundary of the steady flight envelope

Statistic	Symbol	Estimated value	Simulated value	Units
Variance	$\sigma_{v_t}^2$	15	13	ft^2/s^2
Logarithmic residence time	$\hat{\mu}$	2.3	2.5	
Residence time	$\bar{\tau}$	100	96	Seconds
Frequency of exceedance	N	0.0099[a]	0.049	Upcrossings per second
Frequency of upcrossings of mean	N_0	0.10[a]	0.57	Upcrossings per second

[a]Estimated as described in [3].

The stall speed of a Navion at 16,500 ft is 94 ft/s, which is 8 ft/s below the chosen reference true airspeed. Also note that, at 16,500 ft, the maximum steady flight airspeed of a Navion is 230 ft/s. So, if the hypothetical LTI system output y of Sec. II–IV represents the true airspeed perturbations, $y_{\min} = 8$ ft/s and $y_{\max} = 128$ ft/s, and the stall boundary is substantially closer to the reference flight state. Figure 1 depicts the steady flight envelope and the reference steady flight state. The horizontal error bar for the reference steady flight state, which spans the entire width of the flight envelope at 16,500 ft, marks the upper and lower thresholds of the true airspeed. The figure also shows the reference state used to determine the Navion stability derivatives. The second column of Table 1 gives computed results for the various metrics presented in Secs. III and IV. The residence time and probability per unit time require computation of N_0 based on the guidelines given by Hoblit [3]. The integral in the denominator of Eq. (6) is found to converge to 98% of its value at $f = 0.66$ Hz, which is used as the upper bound for the integral in the numerator.

While a flight envelope excursion every 100 s may seem frequent, the duration of each excursion is also important for a hazard like stall because stalls do not develop instantaneously. The true airspeed of the given flight state is 2.2 standard deviations above the stall speed; therefore, the true airspeed exceeds the steady flight envelope 1.3% of the time [2]. Given the residence time and this percentage of time, the duration of each flight envelope excursion is on the order of 1 s, which may be enough time for a stall to develop.

On the normal load factor boundaries of the steady flight envelope, even very brief excursions can be hazardous because the airplane structure can fail relatively quickly. As in the authors' prior work [2], the results of this Note can be readily extended to the load factor boundary. In general, for hazards that do not pose a threat instantaneously, analysis of both the dimensional and dimensionless probabilistic measures of safety gives a more complete picture of the probability of encountering the hazard by allowing an estimate of the duration of the exposure to the hazard.

VI. Simulation of a Navion in Turbulence

This section presents simulation results for a Navion in moderate turbulence to validate the numerical results in the preceding section. The simulation generates sample paths in Simulink for the Navion true airspeed in level longitudinal flight in moderate turbulence. The safety margins described earlier are computed for each sample path and averaged. Figure 2 shows an example of a time history of the true airspeed of the simulated Navion along with a dotted line for the stall speed.

As expected, the mean of the true airspeed is 102 ft/s. The variance of the true airspeed is 13 ft^2/s^2, 13% below the estimated value. The logarithmic residence time is 8.7% above the estimate. The residence time shows even better agreement, while the frequency of exceedance and coefficient N_0 have poor estimates.

According to the model of Sec. III, which is based on Hoblit's frequency of exceedance analysis [3], the residence time should equal the mean interarrival time of the stall speed upcrossings. The mean interarrival time is the reciprocal of the frequency of exceedance, so

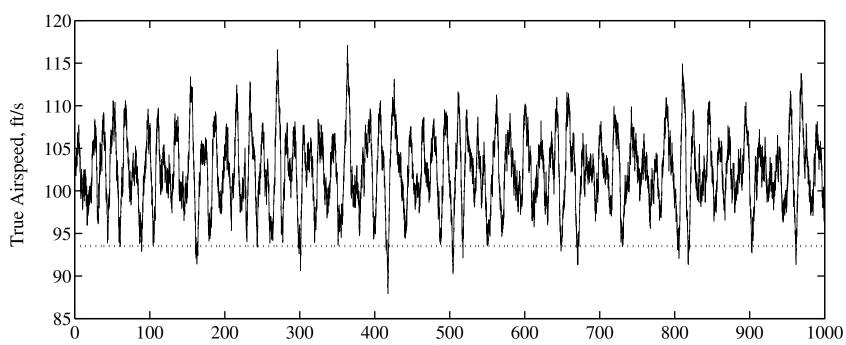

Fig. 2 Example of a time history of the Navion true airspeed in moderate turbulence. The dotted line marks the stall speed.

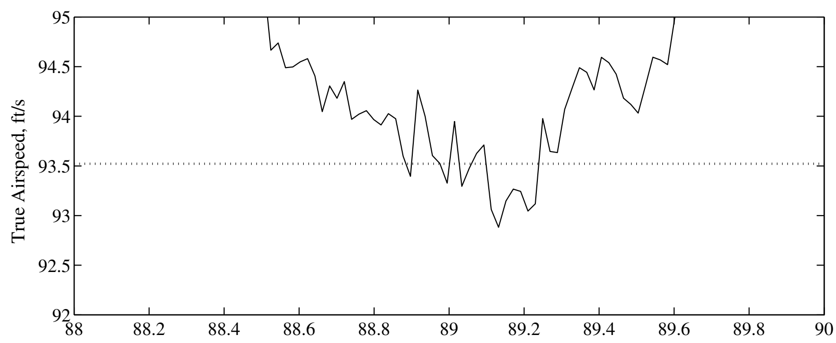

Fig. 3 Close-up of the stall boundary excursion at 90 s in Fig. 2.

these two times are not equal in the simulation. The high simulated values of the frequency of exceedance and N_0 indicate a high-frequency component of the true airspeed perturbations not captured in Sec. III, but one that does not affect the residence time.

Returning to Fig. 2, the true airspeed appears to drop below the stall speed roughly every 100 s on average. However, for a few seconds after crossing the stall boundary, the true airspeed lingers near the boundary and crosses it several more times in rapid succession before reverting to the mean. This is illustrated in Fig. 3, which is a close-up view of the stall boundary excursion at the time 90 s in Fig. 2. A similar phenomenon occurs near the mean, explaining the discrepancy in N_0. Though not presented, smoothing the simulated true airspeed with a low-pass filter can reconcile the estimated and simulated values of N and N_0 without significantly changing the residence time.

Overall, the estimates give good predictions of true airspeed variance, logarithmic residence time, and residence time. The estimates can also give good predictions of the frequency of exceedance if the high-frequency variations of the true airspeed when it is close to the stall boundary are ignored. Both the model and simulation lead to the same analysis of the aircraft's risk exposure: on average, excursions across the stall boundary occur roughly every 100 s and are 1 or 2 s in duration. Such frequent excursions are far from meeting Federal Aviation Administration (FAA) guidelines on probabilities per flight hour [9], but these FAA guidelines refer to probabilities of failure; and flight envelope excursions, especially brief excursions across the stall boundary, do not necessarily correspond to failures.

VII. Conclusions

This Note expands upon the safety margins presented previously by the authors [2] to include probabilities per unit time of exceeding the flight envelope, residence times within the flight envelope, and logarithmic residence times within the flight envelope. To compute these new safety margins, this Note presented extensions of work by Hoblit [3] on frequency of exceedance and probability per unit time and showed them to give the same logarithmic residence time as work by Meerkov and Runolfsson [4,15] on residence times for large deviations of dynamic, stochastic systems. By connecting these various statistics describing stochastic processes, this Note provides a more comprehensive set of metrics to quantify the safety of flight in turbulence and set limits for airplane design and control.

In the authors' prior work [2], the adjustment to the steady flight envelope to form the stationary flight envelope was based on dimensionless measures of exceeding the flight envelope, such as the logarithmic residence time or the number of standard deviations between the mean flight state and the steady flight envelope boundary. Alternative stationary flight envelopes can be formed using dimensional measures, such as the residence time or the probability per unit time. For example, the stationary flight envelope could be the set of steady flight reference states where the residence time for the true airspeed to exceed the steady flight envelope is greater than a certain number of minutes. However, for a hazard like stall, analysis of both the dimensional and dimensionless metrics offers the greatest insight, allowing estimates of both how often and how much time the airplane spends outside the stall boundary of the steady flight envelope.

Acknowledgments

This work was supported in part by the U.S. Department of Defense under U.S. Air Force grant number FA 8650-07-2-3744 and through the National Defense Science and Engineering Graduate Fellowship Program.

References

[1] Belcastro, C. M., and Foster, J. V., "Aircraft Loss-of-Control Accident Analysis," AIAA Paper 2010-8004, 2010.

[2] Richardson, J. R., Atkins, E. M., Kabamba, P. T., and Girard, A. R., "Envelopes for Flight Through Stochastic Gusts," *Journal of Guidance, Control, and Dynamics*, Vol. 36, No. 5, 2013, pp. 1464–1476. doi:10.2514/1.57849

[3] Hoblit, F. M., *Gust Loads on Aircraft: Concepts and Applications*, AIAA, Washington, D.C., 1988, Chap. 4, App. E.

[4] Meerkov, S. M., and Runolfsson, T., "Aiming Control," *Proceedings of the 25th Conference on Decision and Control*, IEEE, Piscataway, NJ, 1986, pp. 494–498.

[5] Richardson, J. R., "Quantifying and Scaling Airplane Performance in Turbulence," Ph.D. Thesis, Univ. of Michigan, Ann Arbor, MI, 2013, pp. 25–38.

[6] "Dryden Wind Turbulence Model (Continuous)," MATLAB Reference Pages, MathWorks, Natick, MA, 2010.

[7] "Von Kármán Wind Turbulence Model (Continuous)," MATLAB Reference Pages, MathWorks, Natick, MA, 2010.

[8] "Flying Qualities of Piloted Aircraft," U.S. Dept. of Defense MIL-STD-1797A, 1990, pp. 673–695, App. A.

[9] "Advisory Circular: System Safety Analysis and Assessment for Part 23 Airplanes," Federal Aviation Administration AC 23.1309-1E, Washington, D.C., 2011.

[10] Bacchi, B., and Ranzi, R., "On the Derivation of the Areal Reduction Factor of Storms," *Atmospheric Research*, Vol. 42, Nos. 1–4, 1996, pp. 123–135. doi:10.1016/0169-8095(95)00058-5

[11] Wesson, R. L., and Perkins, D. M., "Spatial Correlation of Probabilistic Earthquake Ground Motion and Loss," *Bulletin of the Seismological Society of America*, Vol. 91, No. 6, 2001, pp. 1498–1515. doi:10.1785/0120000284

[12] Rice, S. O., "Mathematical Analysis of Random Noise," *Bell System Technical Journal*, Vol. 24, No. 1, 1945, pp. 46–156. doi:10.1002/(ISSN)1538-7305c

[13] Leadbetter, M. R., Lindgren, G., and Rootzén, H., *Extremes and Related Properties of Random Sequences and Processes*, Springer–Verlag, New York, 1983, pp. 176, 238, 260.

[14] Feller, W., *An Introduction to Probability Theory and Its Applications*, 3rd ed., Vol. 1, Wiley, New York, 1967, pp. 446–448.

[15] Meerkov, S. M., and Runolfsson, T., "Output Aiming Control," *Proceedings of the 26th Conference on Decision and Control*, IEEE, Piscataway, NJ, 1987, pp. 1734–1739.